# Self-Powered Gesture Recognition with Ambient Light

**Yichen Li[†], Tianxing Li[†], Ruchir A. Patel, Xing-Dong Yang, and Xia Zhou**
[†]Co-Primary Authors
Department of Computer Science, Dartmouth College
{yichen.li; tianxing.li.gr; ruchir.a.patel.gr; xia.zhou; xing-dong.yang}@dartmouth.edu

## ABSTRACT

We present a self-powered module for gesture recognition that utilizes small, low-cost photodiodes for both energy harvesting and gesture sensing. Operating in the photovoltaic mode, photodiodes harvest energy from ambient light. In the meantime, the instantaneously harvested power from individual photodiodes is monitored and exploited as a clue for sensing finger gestures in proximity. Harvested power from all photodiodes are aggregated to drive the whole gesture-recognition module including a micro-controller running the recognition algorithm. We design robust, lightweight algorithm to recognize finger gestures in the presence of ambient light fluctuations. We fabricate two prototypes to facilitate user's interaction with smart glasses and smart watches. Results show 99.7%/98.3% overall precision/recall in recognizing five gestures on glasses and 99.2%/97.5% precision/recall in recognizing seven gestures on the watch. The system consumes 34.6 µW/74.3 µW for the glasses/watch and thus can be powered by the energy harvested from ambient light. We also test system's robustness under various light intensities, light directions, and ambient light fluctuations. The system maintains high recognition accuracy ($> 96\%$) in all tested settings.

## Author Keywords
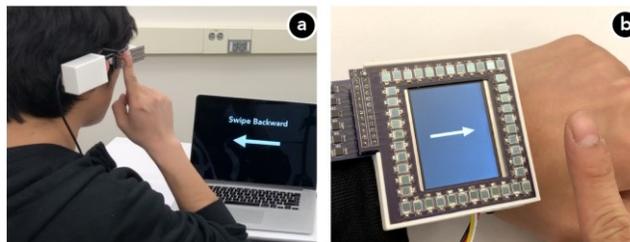Gesture recognition; visible light sensing; energy harvesting.

## INTRODUCTION

Gestural input is essential for interacting with small wearable devices or smart sensors (Internet of Things). Sensing and processing finger gestures, however, consume power. Limiting the energy footprint of gestural input is essential to bringing it to devices with highly constrained energy budget, or without batteries (e.g., battery-less cell phones [50], displays [13,16], cameras [40,41]). Prior studies have explored low-power gesture sensing with various sensing modalities (e.g., electric field, TV or RFID signals, pressure, and capacitance) [9,12,23,53], most requiring on-body sensors dedicated solely to gesture sensing.

**Figure 1: Integrating our prototype with a glasses frame (a) and a watch (b), where arrays of photodiodes harvest energy while being reused for sensing finger gestures.**

In this work, we consider empowering energy-constrained or battery-free devices with energy harvesters for both energy harvesting and gesture sensing. In particular, we exploit ambient light as the sensing medium and energy source for its ubiquity and high energy density[1]. Our approach relies on arrays of small, low-cost photodiodes as energy harvesters while reusing them for always-on recognition of finger gestural inputs (either via touch or in midair near the photodiodes), without the need of battery sources (Figure 1). As the key departure from many existing light-sensing systems [44], photodiodes operate only in the *photovoltaic* mode, thus requiring no input power and only harvesting energy from ambient light [52]. In the meantime, we monitor the instantaneous power harvested by each photodiode and utilize it as the clue to recognize finger gestures. Harvested energy aggregated from all photodiodes powers the whole gesture-recognition module including both its sensing and computation components. Surplus energy[2] can further power other components of the device, which is particularly beneficial for battery-free or ultra-low-power devices.

To develop this approach, the main technical challenge we had to overcome is the uncontrollable ambient light conditions (e.g., light intensity levels, light directions), which often exhibit unpredictable fluctuations caused by user movements or environmental dynamics (e.g., luminary's inherent flickering, clouds passing by, tree leaves waving in the wind). We tackle this challenge using an efficient and

---

[1] The typical energy density of light is 100 mW/cm$^2$ outdoors and 1 mW/cm$^2$ indoors, which is higher than alternative sources (e.g., radio signals, kinetic energy) [11,27,56].

[2] The surplus energy is most significant outdoors, where tens of milliwatts can be harvested under sunlight with 40+ photodiodes (300 mm$^2$ total sensing area).

lightweight recognition algorithm based on constant false alarm rate (CFAR) pulse detection [47]. Without the need of training, the algorithm dynamically estimates current ambient light intensity to ensure that finger movements on or near photodiodes can be reliably detected even under a noisy signal background. Additionally, we exploit the locality of the finger blockage to mitigate the impact of sudden, drastic changes in ambient light (e.g., lights switching off), which by contrast cause global declines in the harvested energy across all photodiodes and thus can be differentiated from the blockage effect of the finger.

We demonstrate our approach using two prototypes, tailored to interactions on smart glasses and smart watches[3]. We optimize the circuit designs to minimize the energy overhead of monitoring the harvested energy from each photodiode. We implement the recognition algorithm on an off-the-shelf micro-controller. With a gesture set of five smart glass gestures and seven smartwatch gestures, we have tested our prototypes extensively under diverse ambient light conditions both indoors and outdoors. Results demonstrate system's ultra-low power consumption (34.6 μW in the smart glass form factor and 74.3 μW in the smartwatch form factor), while achieving 98.9% (SD=1.7) gesture recognition accuracy across all tested lighting conditions.

The main contributions of our work include (1) the concept of a self-powered gesture recognition module, utilizing the harvested energy from photodiodes in the photovoltaic mode for sensing touch and near-range finger gestures; (2) a robust and lightweight gesture recognition algorithm without the need of training; (3) the design and implementation of our system in two wearable form factors; and (4) the results of a series of experiments demonstrating the system's sensing accuracy, energy consumption and harvesting, and robustness in diverse ambient light conditions.
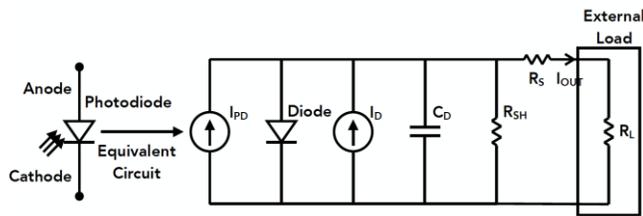
## SENSING PRINCIPLE



**Figure 2: Equivalent circuit of a junction photodiode.**

A junction photodiode bears the intrinsic characteristics of an ordinary signal diode but differs in that it generates a photocurrent when light strikes the junction semiconductor. Figure 2 illustrates the inner working of a junction photodiode with its equivalent circuit, where the generated

---

[3] We choose the watch and glasses as examples only to ease the prototyping. Our approach is generalizable beyond these examples. We plan to integrate our design into battery-free devices as our future work.

photocurrent is denoted as $I_{PD}$, dark current (leakage current) is $I_D$, and $C_D$ denotes the diode's capacitance. The output current, $I_{OUT}$, is a summation of $I_{PD}$ and $I_D$ and can be converted into a voltage, $V_{OUT}$, with a load resistance, $R_L$.

The junction photodiode operates in one of these two modes:

- *Photoconductive mode*, where an external reverse bias voltage is applied to the photodiode and $V_{OUT}$ is linearly proportional to the incoming light intensity. The reverse bias also reduces diode's capacitance $C_D$, thus lowering the diode's response time. This mode is commonly used for sensing light intensity.
- *Photovoltaic mode,* where zero bias (i.e., no input power) is applied and the photodiode generates a more restricted flow of photocurrent depending on incoming optical power. This mode is the basis for solar cells.

Most prior light sensing systems [44] work with photodiodes in the photoconductive mode. It achieves high sensing responsivity at the cost of external power input. By contrast, we focus on diode's photovoltaic mode. It requires no input power while passively harvesting energy from ambient light. Our system's sensing principle stems from the fact that the amount of power harvested by a photodiode ($V_{OUT}$) decreases when a near-field object blocks a part of incoming light. As such, monitoring the output power of the photodiode allows us to detect the blockage of the near-field object. As an example, Figure 3 plots the change in the power harvested by a photodiode when a user swipes the finger twelve times above or on the diode. Here the sensor readings are the output of a 14-bit ADC (maximum value = 16383 for 3.3V). Clearly, as a finger moves in a close range above or directly on an array of photodiodes, it blocks varying subset of photodiodes, causing sharp dips in their harvested power. By monitoring such dips, we can detect the temporal sequence of blocked photodiodes and thus recognize finger's movement direction or touch trajectory.
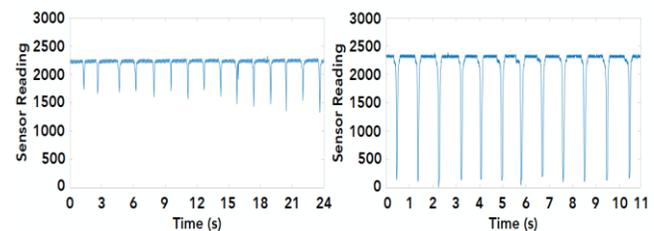


**Figure 3: Time-series of photodiode's harvested power as a finger swipes above it (left) or touches it (right) 12 times.**

Each photodiode is connected to an energy-harvesting circuit for harvesting energy and a voltage-reading circuit, e.g., an analog-to-digital converter (ADC) of a micro-controller, for the system to read the amount of harvested power (voltage) from this photodiode. We periodically switch between the two circuits to facilitate sensing and powering using an ultra-low power CMOS single pole double throw (SPDT) switch. As shown in Figure 4, the analog input of the SPDT connects to the output of the photodiode (anode). SPDT's analog

output port, controlled by a logic input $V_s$, is used for switching between the energy-harvesting circuit and voltage-reading circuit. When $V_s$ is logic HIGH, the photodiode's anode connects to a load resistance, allowing an external ADC to read the converted voltage. When $V_s$ is logic LOW, the photodiode connects to the energy-harvesting circuit, allowing it to harvest energy together with the other photodiodes. Since reading the voltage takes less than 5 μs, its time overhead is negligible. Therefore, the photodiodes are almost completely devoted to energy-harvesting.
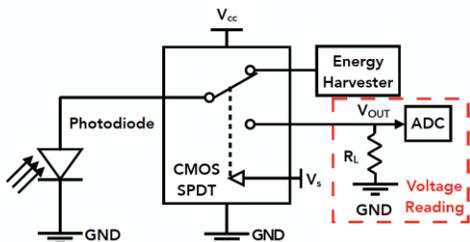


**Figure 4: Circuit design for reading harvested power from individual photodiodes.**

## METHOD

We exploit finger's blocking effect on photodiode's energy harvesting to recognize finger gestures. Next, we introduce the finger gesture set, followed by our recognition algorithm.

### Gesture Set

As shown in Figure 5, we consider twelve gestures for interacting with two example wearable devices (smart glasses and watch). These gestures are chosen from known gesture sets that have been shown to be useful on smart glasses [15] and the watch [2,20,25]. Specifically, there are five glasses gestures including forward and backward swipes in midair, single tap, double tap and double-finger touch. The seven gestures on the watch include swipes in four directions in midair (right, left, up and down), single tap, double tap and double-finger touch. Note that the swipe gestures are designed for performing in midair according to [58].
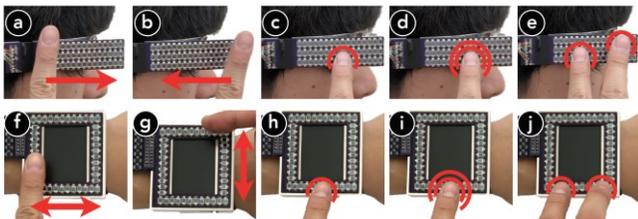


**Figure 5: Gesture set for the glasses (top) and watch (bottom).**

### Gesture Recognition

Recognizing touch is relatively easy, because touching a photodiode almost completely prevents a photodiode from harvesting power (Figure 3), regardless of the ambient light condition. Thus, touch detection can be implemented with a fixed threshold (set as ADC output value 200 in our implementation).

Recognizing midair finger gestures, however, is much more challenging in practice, because its blocking effect is more subject to the impact of uncontrolled ambient light conditions. Figure 6 plots the time series of the power harvested from a photodiode above which a user swiping a finger nine times (see the dips) while walking in a room (300-600 lux). We observe that harvested power fluctuates over time because of the uneven distribution of ambient light intensity. Thus, using a fixed threshold cannot reliably detect the dips to infer midair finger movement. Similarly, using first-order derivatives also renders a poor accuracy because of light flickering and hardware noise[4].
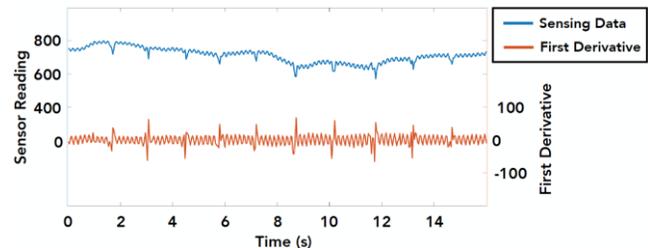


**Figure 6: Time series of the harvested power of a photodiode. The photodiode is carried by a walking user, who swipes a finger above the photodiode nine times.**

To overcome this challenge and enable reliable detection of the occurrences of midair finger blockage at each photodiode, we design a lightweight algorithm based on constant false alarm rate (CFAR). CFAR detection has been widely used in the radar system to detect pulses with a constant false alarm rate in noisy environments [47]. In brief, it estimates the current noise using $m$ observations around the current measurement. It discards $n$ samples adjacent to the current measurement to avoid current measurement polluting the noise estimation. CFAR is the best fit in solving our problem because with adaptive thresholding, it is robust against environmental noises. Additionally, it entails a negligible computation overhead without the need of any signal smoothing process on the raw sensing data.

Unlike the traditional CFAR algorithm that samples references before and after the current measurement, we only consider $m$ reference samples before the current measurement at time $t$ for each photodiode $i$. Let $R^i$ be a vector of prior readings from photodiode $i$ after removing $n$ readings adjacent to the latest reading, where $R^i = \{s^i_{t-m-n}, s^i_{t-m-n+1}, \ldots, s^i_{t-n-1}\}$ and $s^i_t$ is the reading of $i$ [th] photodiode at time $t$. Then, a pulse (i.e., midair blockage) is detected at photodiode $i$ if the following condition holds:

$$\left(s^i_t - \text{mean}(R^i)\right) > \alpha \cdot \left(\text{mean}(|R^i - \text{mean}(R^i)|)\right) \quad (1)$$

---

[4] We have also tested various smoothing techniques [39] to reduce noises. These techniques, however, either reduce the signal-to-noise ratio or entail computational overhead unaffordable by the harvested power.

$\alpha$ is a threshold factor computed as below [42],

$$\alpha = f^{-1}(1 - P_{fa})/f^{-1}\left(\frac{1}{2}\right),$$

where $f$ is the error function, and $P_{fa}$ is the false alarm rate. In our implementation, we set $m$, $n$, and as 16, 8, and 7‰, respectively. $f$ is set as a Gaussian error function based on our measurements.

Since the noise estimation is based on a few reference samples (e.g., 16), the estimation results may not be accurate when ambient light drastically changes within these reference samples. Such sudden ambient light change, however, leads to a global change (drop or rise) in the harvested power across all photodiodes. By contrast, a finger blocks only a subset of photodiodes. Thus, once we detect pulses at all photodiodes, we can infer that a global light change occurs. If it is a global increase in light intensity, then the photodiode experiencing the largest increase is not blocked by the finger and its change reflects the ambient light change $\Delta L$. If it is a global decrease, then the photodiode with the smallest decrease is not blocked by the finger and hence its change reflects $\Delta L$. We then subtract $\Delta L$ from all reference samples before the sudden light change so that the finger blockage can be correctly detected.

After detecting each photodiode's blockage status, we next aggregate their statuses to recognize finger midair gestures. Specifically, we consider finger gestures along N sides of a device (e.g., $N = 4$ for a watch bezel and $N = 1$ for a glasses frame). For each side with photodiodes, we compute the maximal light intensity change as below:

$$L_u = \max_{j \in P_u}(l_j),$$

where $l_j = \begin{cases} |s_t^j - \text{mean}(R^j)|, & \text{if condition (1) holds} \\ 0, & \text{otherwise} \end{cases}$

A potential gesture frame (either touch or midair) is detected if any side is larger than zero. For a non-gesture frame, all sides remain zero. We leverage $Q$ continuous gesture frames that contain maximal light intensity changes for gesture recognition. To do so, we first compute the accumulated light intensity change for each side of the device. We then recognize the side on which the gesture is performed by identifying one with the maximal. Finger's movement direction can then be determined based on the index of the first and last blocked photodiode within the $Q$ gesture frames.

To ensure energy efficiency, we set nonuniform sampling rates across photodiodes. For midair gestures, we only acquire the voltage information from a small set of photodiodes, as the blockage information is sufficient to derive finger midair motion above the photodiodes. In this case, voltage data is sampled at a higher frequency (35 Hz), since midair gestures are performed fast (e.g., less than 0.1s) and the duration of the finger moving across a photodiode can be as short as tens of milliseconds. In contrast, identifying the photodiode(s) that are in contact with the finger(s) requires reading from every photodiode. However, since swiping across a photodiode using touch is slower (e.g., 50 ms) than in the midair, the sampling rate can be lower (17 Hz in our implementation).
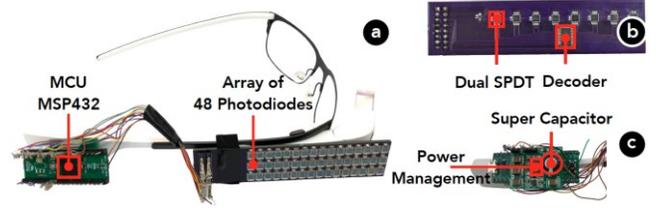


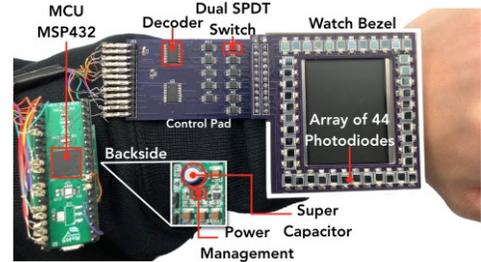Figure 7: Integrating the prototype with Google Glass.



Figure 8: Integrating the prototype with a smart watch.

## PROTOTYPES

We build two prototypes using off-the-shelf hardware, considering interaction with smart glasses and a smart watch as examples (Figure 7 and Figure 8). Note that the watch screen in Figure 8 is only for visualizing the recognition results from our prototype and it is powered by an external power supply. Each prototype consists of arrays of photodiodes, control circuits for switching between energy harvesting and voltage reading, and a micro-controller. Figure 9 illustrates the schematic. We next explain each component in detail.

### Photodiodes and Control Circuits

We choose off-the-shelf silicon PIN photodiodes (Osram BPW34 [66]), providing 21% energy conversion efficiency and measured $2.7 \times 2.7$ mm in size. Photodiodes can be wired in series or in parallel. The output voltage is equal to the summation of each photodiode in the former, and the minimum voltage across photodiodes in the latter. In our experiment, each photodiode provides 350 mV (900 nm, 1 mW/cm$^2$) output voltage. It is below the start voltage of our energy harvester, which is 850 mV without a backup source (e.g., super-capacitor) and 300 mV with a backup source. Therefore, we connect multiple (2 or 3) photodiodes in series as a unit and then connect these units in parallel (as shown in Figure 9). The total harvested power remains the same, independent of how the photodiodes are wired.
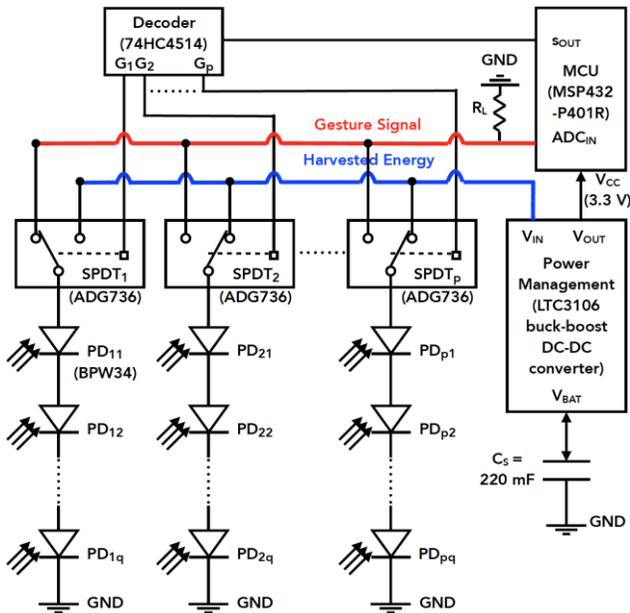
**Figure 9: Schematic of our prototype, where *q* photodiodes are wired in series as a group connecting to a switch, and *p* photodiode groups are wired in parallel, connecting to the power management, decoder, and micro-controller.**

We choose an ultra-low power dual SPDT switch (ADG 736 [67]) to link the photodiode to an energy harvester or ADC. ADG 736 has two SPDT units and can control two photodiodes respectively. SPDT units are controlled by a low-power 16-channel decoder (74HC4514 [68]).

We design and fabricate printed circuit boards (PCB) to host photodiodes and control circuits. For the smart glasses, the PCB board is a thin (1.6 mm) two-layer board that hosts 16 × 3 photodiodes on the front and control circuits on the back (Figure 7). Three photodiodes in a column form a unit, controlled by a SPDT switch on the back. The PCB is attached to the side arm of a Google Glass. For the smart watch, we fabricate two customized PCBs (Figure 8). The first PCB is a two-layer board that hosts 44 photodiodes and two photodiodes form a unit, providing 22 channels for reading harvested voltages. This PCB surrounds the watch screen and its outputs connect to the second board, which is a 4-layer PCB with 11 duel SPDT switches and two 16-channels decoders. The additional decoder only requires one more port from micro-controller.

For both prototypes, all units are used for detecting touches while a subset of units are used for detecting midair gestures. Specifically, only 4 units (column 1, 5, 9 and 13) are used in the glasses scenario while 11 units uniformly sampled are used in the watch scenario.

The harvested power fluctuates due to user's mobility and ambient light variations. To maintain a stable power output, our power management component is a buck-boost DC/DC converter (LTC3106 [69]) combined with a super-capacitor (0.22 F) as shown in Figure 9. The super-capacitor stores surplus energy to supply the system when the harvested energy is lower than the requirement (e.g., in low light conditions).

**Micro-Controller**
We use an ultra-low-power micro-controller (MINI-M4 for MSP432 board [70]) to control the decoder, digitize output voltage of each photodiode and recognize finger gestures. We use the MSP432P401R micro-controller in three modes [71]: 1) LPM3 mode (660 nA/3.3V, CPU idle); 2) active mode (80 µA/MHz/3.3V, 48 MHz clock) running CFAR; and 3) ADC_DMA mode (1.4 mA/3.3V, 25 MHz clock) controlling the decoder and sampling voltage number. The micro-controller is in the active mode for 0.14% (glasses) and 0.36% (watch) of the time, in the ADC_DMA mode for 0.28% (glasses) and 0.39% (watch) of the time, and in the LPM3 mode otherwise. Given that an ADC conversion takes 5 µs, collecting voltage numbers from all units takes 80 µs on the glasses and 110 µs on the watch. Thus, photodiodes harvest power in more than 99.5% of the time.

The micro-controller runs the gesture recognition algorithm to output detected gesture. Our measurements show that the recognizing a gesture takes 10 µs on the glasses prototype and 30 µs on the watch. To minimize the power consumption, we remove unrelated units (e.g., USB bridge chip and LED indicators) on the board. To further reduce the computation overhead, we replace all of the multiplications and divisions to shift operations, since the multipliers and dividers are factor of two. The energy harvested by photodiodes powers the whole system, including SPDT switches, decoders and the micro-controller.

## STUDY 1: RECOGNITION ACCURACY
We begin with examining gesture recognition accuracy.

**Participants**
Ten participants (9 males, age: min=20, max=33, mean=24.2) were recruited in this study. All of them are right-handed. The diameters of participants' index fingers range from 12 mm to 17.5 mm (SD = 1.5) and that of the middle fingers are between 12.5 mm and 17 mm (SD = 1.1).

**Data Collection**
Data collection is carried out in an office room (4.5 m × 5.6 m), which has 6 fluorescent lights on the ceiling. Participants perform the task in a sitting position at a desk, 2 m below the ceiling. Light intensity is measured using a LX1330B light meter. We found the average light intensity around the photodiodes of the glasses is between 472 and 544 lux (SD = 21.1), depending on the participant's height. The light intensity at the watch face is between 860 and 933 lux (SD = 23.9), depending on the position of participants' hand.

Prior to the start of the study, participants are given several minutes to practice the gestures. During the study, participants perform the gestures using the right hand in their normal speed. In the watch scenario, participants rest the left arm on the desk and use the right hand to perform the

gestures. For both the watch and glasses, touch is performed directly on the photodiodes whereas midair gestures are performed with the finger at roughly 0.5 cm to 3 cm distance to the photodiodes. Each gesture is repeated 20 times. A five-minute break was given between the glass and watch scenarios. In total, we have collected 2400 gesture instances (10 participants $\times$ 12 gestures $\times$ 20 repetitions) for analysis.

### Result

Recognition accuracy is measured using *precision* and *recall* [6]. *Precision* is the percentage of the correctly recognized gestures among all the detected gestures. *Recall* is the percentage of the correctly recognized gestures among the entire gesture set (e.g., 20 for each gesture in our dataset).

The precision and recall for the glasses is 99.7% and 98.3%, respectively. The precision and recall for the watch is 99.2% and 97.5%, respectively. Figure 10 shows the result per participant and the precision and recall averaged across all the participants as the 'overall' bar. The recall rate for P6 is the lowest. This is because P6 occasionally performs the gestures more than 3 cm away from the photodiodes, resulting into incorrect recognitions of some midair gestures.
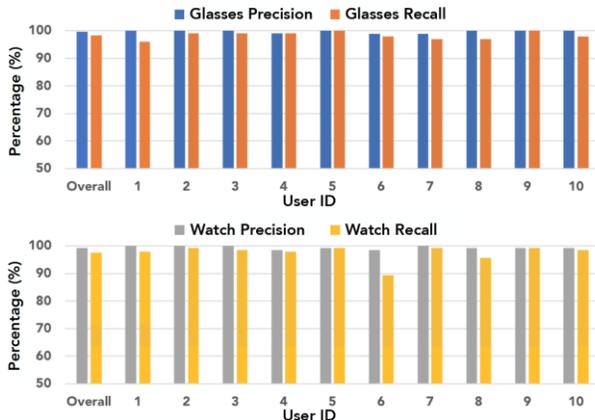


**Figure 10: Precision and recall of gesture recognition across participants.**

Recognition accuracy across different gestures is shown in Figure 11. As expected, touch gestures (e.g., tap) receive the highest accuracy (precision = 99.5%, recall = 99.5%). This is primarily attributed to the significant impact of touch on harvested energy. When a finger touches the photodiodes, the energy harvested from the photodiode drops to somewhere near zero (not zero due to the dark current) allowing the gestures to be easily detected. The recognition accuracy of midair gestures is higher with the glasses than the watch, where the precision/recall is 100%/96.5% for the glasses and 99.5%/96.1% for the watch. This is partially because the glasses has a smaller set of 1D gestures whereas the gesture set for the watch is larger, including both 1D and 2D gestures. We will discuss how to improve the glasses prototype to sense 2D finger gestures in the future work.

We also analyze the impact of gesture speed on recognition accuracy. From the results of participants gesturing in various speeds, we do not observe noticeable differences in accuracy caused by gesture speed. The reason is that given the length of the photodiode array (7.1 cm for the glasses, 5.4 cm for the watch) and the ADC rate (35 Hz), the fastest swiping speed the system can handle is 245 cm/s (glasses) and 189 cm/s (watch), far above our normal gesture speed. Thus, the system maintains its recognition accuracy under various normal speeds of gesturing.
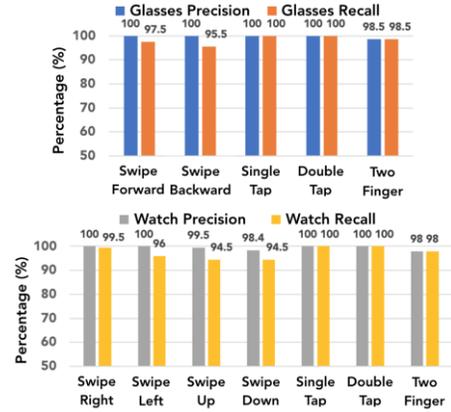


**Figure 11: Recognition accuracy across finger gestures.**

### STUDY 2: POWER CONSUMPTION AND HARVESTING

We next examine the power consumption of our prototypes and their ability to harvest energy in various ambient light conditions.

### Power Consumption

We measure the power consumption of our prototypes using a Monsoon power monitor [72], averaged over 10-second intervals for five testing rounds. As shown in Table 1, the overall power consumption for gesture recognition is 34.6 µW for the glasses and 74.3 µW for the watch. The watch consumes more power because the device has more photodiodes. The gesture set of the watch contains more 2D gestures that entail slightly higher computational overhead to recognize. For both prototypes, 94-95% of the power is consumed by the micro-controller running the recognition algorithm and by the built-in ADC acquiring voltage data (30-40% of the power). The micro-controller consumes less than 5 µW in the sleep mode (LPM3 mode) when no gesture is detected. It is possible to replace the ADC with ultra-low-power comparators (e.g., TS881 [73]) to further improve energy efficiency. Moreover, the photodiodes do not consume any power and their control circuits (e.g., SPDT switches, decoder) also consume negligible power.

**Table 1: Breakdown of power consumption for two prototypes.**

|         | MCU-ADC | MCU-Recognition | Control Board | In Total |
|---------|---------|-----------------|---------------|----------|
| Glasses | 13.6 uW | 19.2 uW         | 1.8 uW        | 34.6 uW  |
| Watch   | 22.5 uW | 48.3 uW         | 3.5 uW        | 74.3 uW  |

### Energy Harvesting

We also conduct a study to measure the amount of energy our prototypes can harvest in various ambient light conditions. A participant (188 cm tall) is recruited for the

study, where participant is asked to wear the devices in a sitting and standing position. The amount of the energy harvested by the devices is measured in four indoor lighting conditions and three outdoor lighting conditions. The indoor lighting conditions include: 1) a dark room (200 lux); 2) normal office lighting (600 lux); 3) bright lab condition (1K lux), and 4) next to a lab window during noon (2K lux). The outdoor lighting conditions include: 1) in the shadow of a tall building (4K lux); 2) under direct sunlight in a cloudy day (20K lux), and 3) under direct sunlight in a sunny day (110K lux). When standing, participant is asked to occasionally raise the wrist to the front of the chest to mimic the situation where a user is interacting with the device with photodiodes facing the sky or ceiling. When the wrist is not held in front of the chest, photodiodes face outside the body. When sitting, participant rests the arm on a table of 70-cm height.

Table 2 shows the results of all the tested conditions. In the indoor conditions, the power harvested by our devices ranges from 23 µW to 124 µW. Even though the glasses prototype contains more (48) photodiodes than the watch, it harvests slightly less power in most conditions because the light to the glasses often comes from larger incident angles. In the outdoor conditions, the amount of power harvested by both devices is significantly higher, ranging from 1.3 mW to 46.5 mW. This is because sunlight contains more infrared light, which photodiodes can convert to energy more efficiently. Overall, our result shows that the energy harvested by our prototypes is sufficient to power the entire gesture recognition module except when participant is in the sitting position in the dark room. This problem can be mitigated by the supercapacitor in our prototypes, with which surplus energy harvested in other conditions is stored to power the system in situations when the harvested energy is insufficient. Filling in this power gap (11 - 33 µW) for one hour needs a user to stay outdoors for 26 - 91 seconds in shadow, or 5 - 15 seconds in a cloudy day (20K lux) or 1 - 3 seconds under direct sunlight (110K lux).

**Table 2: Harvested energy in various ambient light conditions.**

| Light Condition (lux) | Indoor | | | | Outdoor | | |
|---|---|---|---|---|---|---|---|
| | Dark Room (200) | Normal Office (600) | Bright Lab (1K) | Near Window (2K) | Shadow (4K) | Cloudy (20K) | Direct Sunlight (110K) |
| Glasses Sitting | 23 uW | 48 uW | 62 uW | 332 uW | — | — | — |
| Glasses Standing | 44 uW | 89 uW | 115 uW | 346 uW | 1.5 mW | 8.6 mW | 46.5 mW |
| Watch Sitting | 41 uW | 76 uW | 110 uW | 306 uW | — | — | — |
| Watch Standing | 62 uW | 91 uW | 124 uW | 315 uW | 1.3 mW | 7.8 mW | 41.8 mW |

## STUDY 3: SYSTEM ROBUSTNESS

Finally, we examine system robustness against diverse ambient light conditions. Since recognizing touch is quite robust (e.g., 99.5% for both precision and recall) against all the tested conditions, we only tested midair gestures in this study. In each of the tested lighting condition, we have

collected 100 gesture instances (5 gestures $\times$ 20 repetitions) for the glasses and 140 gesture instances (7 gestures $\times$ 20 repetitions) for the watch. Next, we present our results.

**Stable Ambient Light**
We first test our devices under a stable ambient light condition, i.e., no sharp change in light intensity. We examine the impact of the intensity and direction of ambient light on recognition accuracy.

*Varying Intensity Level*
We test six different levels of light intensity, including three indoor conditions: dark room (200 lux), normal office (600 lux) and bright lab (1K lux), and 3 outdoor conditions: under shadow (4K lux), under cloud (20K lux) and direct sunlight (110K lux). We also test the watch prototype with no ambient light (0 lux). In this condition, our systems rely on the screen light reflected by the finger.

Figure 12 plots the results. Both prototypes achieve high precision (100%) and recall (99.8%) in the indoor conditions. The precisions for the outdoor conditions are slightly lower (94.9% for the glasses and 97.5% for the watch because of higher fluctuated noises from sunlight. As for the case with no ambient light, the devices achieve a precision of 100%, solely depending on the screen light reflected from the finger. In this case, the CFAR method detects power rises, instead of dips to identify the blocked photodiodes for gesture recognition. The recall for the no-light condition is slightly lower (90%) because the intensity of the reflected light is not sufficient enough to guarantee a significant impact on the harvested energy. Overall, our result suggests that CFAR is effective for detecting the tested finger gestures in various levels of ambient light intensity.

*Varying Light Direction*
We also test the robustness of our system under varying light directions. In this study, we vary the direction of incoming light using a floor lamp. For the glasses, we place the lamp at three angles to the photodiodes (-45°, 0° and +45°). When the lamp is placed at 0° angle, it faces directly to the photodiodes. For the watch, we placed the lamp in four
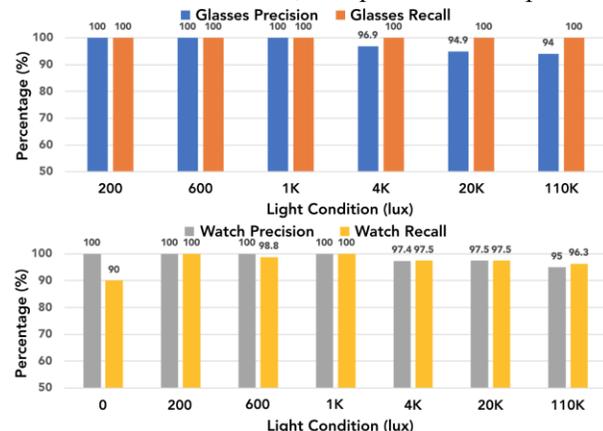


**Figure 12: Accuracy of gesture recognition under different levels of ambient light intensity.**

directions (Forward, Left, Right and Above). Light intensity on the watch face is around 300 lux.

Figure 13 summarizes the results for both prototypes. The gesture recognition accuracy for the glasses remains high (98.1% precision and 99.2% recall) across all directions, since the direction of the incoming light has little impact on the sequence in which the 1D array of photodiodes are blocked. The watch receives slightly lower recall (96.3-98.8%) when the light comes from the Left or Right. This is because the shadow of the finger occasionally lands outside the photodiodes when the finger swipes up or down. In this case, the system does not sense any voltage change. The same effect appears when swiping the finger left or right with the light coming from Front. Additionally, when light comes from the right side of the device, the shadow of the moving finger can affect certain photodiodes and interfere with the sensing of finger motion, and vice versa for left-handed users. Overall, our results show that both prototypes can maintain high precision/recall in all the tested lighting directions.
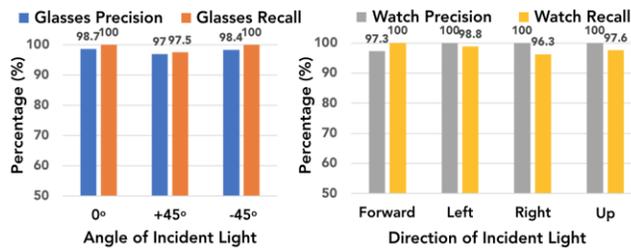


**Figure 14: Accuracy of gesture recognition under ambient light in varying directions.**

**Dynamic Ambient Light**
We then test our prototypes in a more challenging scenario, where the ambient light fluctuates. We examine five possible causes for light fluctuation, including luminary flickering, partial light blockage, moving shadow from a nearby people, sudden global light change, and user movement. Figure 14 summarizes the results for all scenarios.

*Flicker Effect*
The flicker effect appears in some indoor luminaries driven by alternating current. In this study, we test our prototypes in two offices (light intensity around 600 lux), each has a flickering luminary one flashing at approximately 60 Hz and another one at 120 Hz. The flicker frequency is measured by an OWON oscilloscope. Figure 14 shows that the prototypes achieve 100% precision and 97-98% recall. It demonstrates that our CFAR method can effectively remove the high-frequency flickering signals and precisely detects the photodiodes blocked by the nearby finger in the midair. A light flickering at around 30 Hz can significantly affect performance of our system since it is close to our sampling rate (35 Hz). However, 30 Hz flickering light is rare in the indoor environments because it is noticeable by naked eyes.

*Partial Light Difference*
We then test situations where the photodiodes are exposed to nonuniform light intensities. We place a polarizer on the
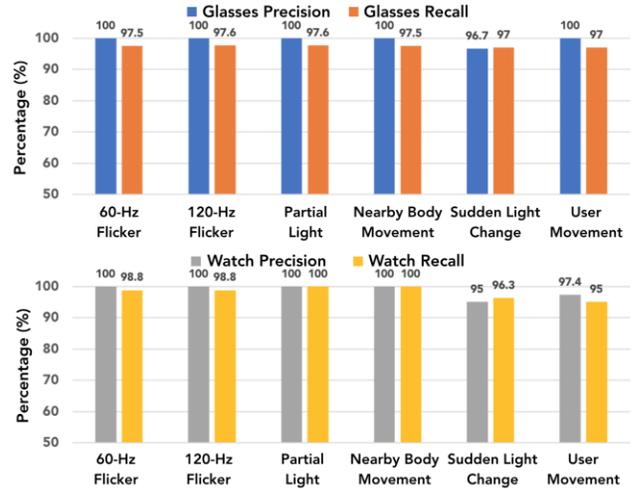


**Figure 13: Accuracy of gesture recognition under ambient light fluctuations.**

prototypes, resulting half of the photodiodes under 900-lux while the other half under 400 lux. As shown in Figure 14, the precision and recall remain 100% and 98%, respectively. Such high accuracy is primarily because of the CFAR algorithm, where each photodiode uses its own dynamic thresholding. As a result, blockage detection is not affected by the nonuniform light intensity across the photodiodes.

*Nearby Body Movement*
We next test the impact of nearby body movement on recognition accuracy. Someone passing near the user may cast shadow on the photodiodes, thus causing false positives. In this experiment, we recruit another participant as a distractor, who walks in random trajectories near the user wearing the devices or wave the hands 30 cm away from the prototypes. Our result shows that the movement of a nearby person has negligible impact on recognition accuracy. This is because our system's sensing range is approximately between 0.5 cm to 3 cm. A finger in such close distance can block a sufficient amount of light to cause noticeable dips in harvested power. Whereas, objects further away from photodiodes block far less light and have little interference with the gesture sensing.

*Sudden Light Change*
We now examine the impact of drastic, sudden ambient light change on the recognition accuracy. We conduct the experiment in an office illumined by multiple floor lamps. A participant wears our prototypes on at a time when performing the gestures, during which one floor lamp is turned on and off at roughly 1-3 Hz. This introduces quick change of light intensity oscillating between 550 lux and 800 lux measured at the photodiodes. Results show that the systems still achieve high precision (96.7% for glasses and 95% for watch) and recall (97% for glasses and 96.3%). It demonstrates that our method can effectively identify the global light change and subtract it from gesture recognition. As a result, it filters out the sudden global light change and detects midair gesture correctly.

*User Movement*

Finally, we test our prototypes during user movements. A participant performs the gestures with our prototypes when walking in a hallway, where light distributes nonuniformly, ranging between 500 lux and 1K lux. The results show that the glasses prototype achieves 100% precision and 97% recall. The recall accuracy decreases because participant occasionally performs the gestures outside the device's sensing range (e.g., 3 cm). The watch achieves 97.4% precision and 95% recall. Four out of eighty midair gestures are classified incorrectly, possibly caused by the nearby shadows when moving.

## DEMO APPLICATIONS



**Figure 15: Demo applications: (a) a user swipes finger to browse websites (b) a user plays game on smartwatch.**

We implemented two demo applications to showcase our self-powered system's potential on wearable devices. Our first application allows the user to interact with a head-worn display using the midair and touch gestures. We place our glasses frame prototype on a Google Glass's touchpad. With our glasses frame, most of conventional touch gestures can be implemented and additional midair swipe gestures are also supported. More gestures can be added which will be discussed in future work. In addition, our system provides a successful self-powered solution to battery-limited smart devices and it can even power other units on smart devices. In our application, a midair swipe gesture is a shortcut for page turning while browsing websites with smart-glasses （Figure 15 (a)).

Our second application is an additional controller on smartwatch with our watch bezel prototype. We created a smartwatch prototype using a 2" TFT display, a 3D printed case, and our watch bezel. In this application, the user can interact with the smartwatch in midair or touching the bezel. This provides an external and freedom way and has two potential benefits. First, users can set the limited buttons on the original smartwatch for some important functions, such as answering the phone and activating intelligent personal assistant. Other minor function can set on our self-powered watch bezel, such as muting the device and rotating the screen. Second, our system provides a midair solution to extend the interactive area of the screen-limited smartwatch. For example, the user can swipe the finger to play mobile games on the smartwatch (Figure 15 (b)).

## RELATED WORK

We summarize related work in low-power gesture sensing, visible light sensing and midair gesture sensing in general.

## Low-Power Gesture Sensing

Existing studies have explored various sensing modalities for low-power gesture sensing. Examples include innovative sensing with electric fields [9], TV or RFID signals [23], pressure [12] and capacitive [53][5] sensors. In particular, Gabe Cohn et al presented an ultra-low-power method for passively sensing body motion using static electric fields by measuring the voltage at any single location on the body [9]. Its components consume 6.6 µW. WristFlex uses an array of force sensitive resistors to distinguish subtle finger pinch gestures. The sensors alone consume 60.7 µW [12]. Allsee [23] recognizes hand gestures by examining its reflection of existing wireless signals, e.g. TV or RFID signals. Its ADC consumes 27-29 µW. Eliminating ADC by comparators can further drive down the power to 4.57-5.85 µW.

We are inspired by these works. Our design follows a similar spirit and yet considers a different medium. Our sensing component alone (photodiodes and control circuits) consumes lower power (1.8 µW for the glasses and 3.5 µW for the watch) than that of some prior systems [12]. We can consider optimization similar to [23] to eliminate ADC to further reduce power consumption. More importantly, our sensing component also harvests power to drive the whole gesture recognition module including the micro-controller running the recognition algorithm. The high energy density of light allows more energy to be harvested compared to other medium and the surplus energy can drive other components of the device.

## Visible Light Sensing

Active research [44] has studied the use of visible light for indoor localization [4,18,36,60,63], coarse-grained body sensing [30,31,55,65] and LED-based finger tracking [14,19,21,54,62]. For achieving higher sensing accuracy, most systems have used photodiodes in the photoconductive mode. Additionally, most designs require active modulation of the light source. Our work differs in that we use photodiodes in the photovoltaic mode and exploit the changes in harvested power for gesture sensing. Our design works with existing ambient light without the need to modulate the light source.

Photodiode's photovoltaic mode has been exploited by prior works. In [55], Varshney et al pairs a solar cell with a thresholding circuit to sense binary blockage information. It then sends the information via backscatter communication to another machine that runs the gesture detection algorithm. It supports three hand gestures. The sensing and communication consumes 20 µW. With a fixed thresholding circuit, it is challenging for the system to adapt to various ambient light conditions. In comparison, we consider arrays of photodiodes for gestures sensing and design algorithm for robust gesture detection in diverse ambient light conditions. We also build a standalone module that runs the gesture recognition algorithm. The power harvested by photodiodes drives the whole module. In [41], Nayar et al exploit photdiode's photovoltaic mode for both sensing and energy

harvesting and study the feasibility of building self-powered image sensors. We apply the concept for building a self-powered gesture recognition module and fabricate two complete prototypes to demonstrate its feasibility.

## Midair Gesture Sensing

Midair gesture is one of an effective solution to extend the interaction space [1]. A variety of sensing techniques have been developed to detect midair gestures. They have considered the use of cameras [8,10,26,32,34,48,51,57,59], infrared sensors [7,22,25,28,35,43,46,58], WiFi signal [5,45,49,61], GSM signals [64] and other wearable sensors [17,33,37]. Camera-based methods are commonly used by existing products such as Xbox Kinect [74], Leap Motion [75], PointGrab [76] and CrunchFish [77]. These methods often involve higher computational overhead. In comparison, our work detects midair gestures with a much more lightweight algorithm and the gesture recognition module requires no external power input. SideSight [7] and FlexAura [35] require multiple (10 in SideSight, 384 in FlexAura) infrared emitters. Each emitter in SideSight/FlexAura consumes 165/180-mW peak power. Latest infrared proximity sensors (e.g., APDS 9130 [78], APDS 9190 [79]) consume 140-157 µW at 20 Hz sampling rate. In comparison, our system is passively reusing ambient light and powers itself as a complete module.

## DISCUSSION AND FUTURE WORK

In this section, we discuss the limitations of our study, insights gained from this work, and plans for future work.

*Enriching Sensing Capabilities.* As a proof of concept, our current prototypes are built for recognizing a small set of simple finger gestures (Figure 5). The system principle, however, can be extended to recognize a richer set of gestures. Touch-related gestures can be expanded by including multi-touch, rotating or sliding fingertips on the photodiodes. These gestures can be used to create self-powered interaction buttons on any energy-limited devices. As for midair gestures, we will consider adding finger drawing various shapes (e.g., circle, rectangle, triangle, tick, cross) or numbers. We will examine various lightweight machine learning algorithms (e.g., kNN, boosted trees) to classify these more sophisticated movement trajectories. These learning models can be trained with data collected across participants. We will start collecting data and examine the feasibility. Furthermore, current midair gestures mainly differ in finger movement direction. Moving forward, we plan to examine inferring movement distance based on the sequence of blocked photodiodes. The recognition of movement distance can enable finer-grained input control, e.g., tuning down/up volume, adjusting screen brightness. Moreover, our current glasses prototype recognizes only the horizontal movement of a midair finger, because the photodiodes in each vertical column are connected in series as a unit, mainly to ease the arrangement of SPDT switches on the back of the circuit board. We will further optimize our circuit design and connect fewer photodiodes in series to

sense vertical movement. It can enable a richer set of finger gestures to interact with the glasses.

*Hardware Optimization.* The power consumption of our prototypes can be further reduced with following hardware optimization. *First*, we currently use micro-controller's built-in ADC to ease the programming and debugging. To further reduce power, we will consider the use of external lower-power ADCs, such as ads7042 (< 1 µW at 1 kSPS) [80]. Furthermore, for the recognition of gestures (e.g. touch) requiring fixed thresholding, we can consider replacing ADC with low-power comparators that directly compare analog signals for gesture recognition, similarly to the prior study[23]. It will greatly lower system power given that ADC currently consumes 30-40% of power. *Second*, our current micro-controller is a development board that embeds many units unnecessary for gesture recognition. A customized computing unit with only relevant calculation units can further lower the power consumption of running the gesture recognition algorithm (currently consuming 55-65% of power). *Third*, our current prototypes directly use an internal timer to control the sampling rate. We will consider an external timer to achieve lower power, which has been successfully applied in a prior study [24]. *Finally*, the whole system can be implemented as an integrated circuit with all hardware components, including customized ultra-low power MCU, ADC/comparator units and switches. This can further minimize the total power consumption.

On the energy-harvesting side, the photodiodes (BPW 34) in our current prototypes have 21% energy conversion efficiency, thus an individual photodiode can harvest only a few microwatts under indoor lighting. It results in 44/48 photodiodes needed in our watch/glasses prototypes, contributing to their bulky looks. We can miniaturize the prototype in two directions. First, currently only 39% of the photodiode surface (18 mm$^2$) is used for sensing. Optimizing the fabrication of photodiodes and their arrangement can reduce the actual photodiode array size for harvesting the same amount of power. Second, with advances in the materials of photodiodes and mini solar cells, we can use photodiodes with higher energy conversion ratios. For example, advanced organic solar cells can achieve energy conversion ratio of 50% [3]. It can lead to fewer cells to realize the same functionality or enhanced gesture recognition ability with the same number of cells. Moreover, arrays of more efficient photodiodes can harvest more energy to better support energy-constrained or battery-free devices.

*Other Prototype Examples.* We demonstrate our approach using the smart watch and glasses as two examples only to ease the prototyping. Our approach is generalizable and can be integrated into other types of devices. We are particularly interested in examining the integration of our approach into emerging battery-free systems [13,16,29,40,41,50]. In these systems, energy harvesters are the must-have components and our approach reuses them to simultaneously provide gestural input with minimal additional energy overhead.

# REFERENCES

1. Roland Aigner, Daniel Wigdor, Hrvoje Benko, Michael Haller, David Lindlbauer, Alexandra Ion, Shengdong Zhao, and Jeffrey Tzu Kwan Valino Koh. 2012. Understanding Mid-Air Hand Gestures : A Study of Human Preferences in Usage of Gesture Types for HCI. *Tech. Rep. MSR-TR-2012-11*: 10. Retrieved from https://www.microsoft.com/en-us/research/publication/understanding-mid-air-hand-gestures-a-study-of-human-preferences-in-usage-of-gesture-types-for-hci/

2. Apple. Apple Watch Gestures.

3. Shigeo Asahi, Haruyuki Teranishi, Kazuki Kusaki, Toshiyuki Kaizu, and Takashi Kita. 2017. Two-step photon up-conversion solar cells. *Nature Communications* 8. https://doi.org/10.1038/ncomms14962

4. Shahid Ayub, Sharadha Kariyawasam, Mahsa Honary, and Bahram Honary. 2013. Visible light ID system for indoor localization. *Wireless, Mobile and Multimedia Networks (ICWMMN 2013), 5th IET International Conference on*: 254–257. https://doi.org/10.1049/cp.2013.2419

5. Andreas Braun, Reiner Wichert, Arjan Kuijper, and Dieter W. Fellner. 2015. Capacitive proximity sensing in smart environments. *Journal of Ambient Intelligence and Smart Environments* 7, 4: 483–510. https://doi.org/10.3233/AIS-150324

6. Michael Buckland and Fredric Gey. 1994. The relationship between Recall and Precision. *Journal of the American Society for Information Science* 45, 1: 12–19. https://doi.org/10.1002/(SICI)1097-4571(199401)45:1<12::AID-ASI2>3.0.CO;2-L

7. Alex Butler, Shahram Izadi, and Steve Hodges. 2008. SideSight : Multi- " touch " interaction around small devices. *UIST '08: Proceedings of the 21st annual ACM symposium on User interface software and technology* 23, 21: 201–204. https://doi.org/http://doi.acm.org/10.1145/1449715.1449746

8. Xiang 'Anthony' Chen, Julia Schwarz, Chris Harrison, Jennifer Mankoff, and Scott E. Hudson. 2014. Air+Touch: Interweaving Touch & In-Air Gestures. *Proceedings of the ACM Symposium on User Interface Software and Technology, UIST 2014*: 519–525. https://doi.org/10.1145/2642918.2647392

9. Gabe Cohn, Sidhant Gupta, Tien-Jui Lee, Dan Morris, Joshua R Smith, Matthew S Reynolds, Desney S Tan, and Shwetak N Patel. 2012. An Ultra-low-power Human Body Motion Sensor Using Static Electric Field Sensing. *Proceedings of the 2012 ACM Conference on Ubiquitous Computing*: 99–102. https://doi.org/10.1145/2370216.2370233

10. Andrea Colaço, Ahmed Kirmani, Hye Soo Yang, Nan-Wei Gong, Chris Schmandt, and Vivek K. Goyal. 2013. Mime: Compact, Low-Power 3D Gesture Sensing for Interaction with Head-Mounted Displays. *Proceedings of the 26th annual ACM symposium on User interface software and technology - UIST '13*: 227–236. https://doi.org/10.1145/2501988.2502042

11. M. A. Cowell, B. P. Lechene, P. Raffone, J. W. Evans, A. C. Arias, and P. K. Wright. 2016. Wireless sensor node demonstrating indoor-light energy harvesting and voltage-triggered duty cycling. In *Journal of Physics: Conference Series*. https://doi.org/10.1088/1742-6596/773/1/012033

12. Artem Dementyev and Joseph A. Paradiso. 2014. WristFlex: Low-Power Gesture Input with Wrist-Worn Pressure Sensors. *Proceedings of the 27th annual ACM symposium on User interface software and technology - UIST '14*: 161–166. https://doi.org/10.1145/2642918.2647396

13. Christine Dierk, Molly Jane, Pearce Nicholas, and Eric Paulos. 2018. AlterWear : Battery-Free Wearable Displays for Opportunistic Interactions. In *Proceedings of the SIGCHI Conference on Human Factors in Computing Systems*. https://doi.org/10.1145/3173574.3173794

14. Michal Karol Dobrzynski, Ramon Pericet-Camara, and Dario Floreano. 2012. Vision tape-a flexible compound vision sensor for motion detection and proximity estimation. *IEEE Sensors Journal* 12, 5: 1131–1139. https://doi.org/10.1109/JSEN.2011.2166760

15. Google. Google Glass Gestures. Retrieved from https://support.google.com/glass/answer/3064184?hl=en

16. Tobias Grosse-Puppendahl, Steve Hodges, Nicholas Chen, John Helmes, Stuart Taylor, James Scott, Josh Fromm, and David Sweeney. 2016. Exploring the Design Space for Energy-Harvesting Situated Displays. In *Proceedings of the 29th Annual Symposium on User Interface Software and Technology - UIST '16*. https://doi.org/10.1145/2984511.2984513

17. Sidhant Gupta, Daniel Morris, Shwetak Patel, and Desney Tan. 2012. SoundWave: Using the Doppler Effect to Sense Gestures. *Proceedings of the 2012 ACM annual conference on Human Factors in Computing Systems - CHI '12*: 1911–1914. https://doi.org/10.1145/2207676.2208331

18. Naveed U L Hassan, Aqsa Naeem, and Muhammad Adeel Pasha. 2014. Indoor Positioning Using Visible LED Lights: A Survey. *ACM Transactions on Sensor Networks* 11, 2: 1–24. https://doi.org/10.1145/0000000.000000

19. Steve Hodges, Shahram Izadi, Alex Butler, Alban Rrustemi, and Bill Buxton. 2007. ThinSight. *Proceedings of the 20th annual ACM symposium on User interface software and technology - UIST '07*: 259. https://doi.org/10.1145/1294211.1294258

20. Huawei. Huawei Smartwatch Bezel Gestures.

21. J. Kim, S. Yun and Y. Kim. 2016. Low-power motion gesture sensor with a partially open cavity package. *Opt. Express 24*: 10537–10546.

22. Jun Gong, Yang Zhang , Xia Zhou and Xing-Dong Yang. 2017. Pyro: Thumb-Tip Gesture Recognition Using Pyroelectric Infrared Sensing. In *In Proceedings of the 30th Annual ACM Symposium on User Interface Software and Technology (UIST '17)*, 553–563.

23. Bryce Kellogg, Vamsi Talla, and Shyamnath Gollakota. 2014. Bringing Gesture Recognition To All Devices. *Proceedings of the 11th USENIX Symposium on Networked Systems Design and Implementation (NSDI 14)*: 303–316.

24. Bryce Kellogg, Vamsi Talla, Joshua R. Smith, and Shyamnath Gollakot. 2017. PASSIVE WI-FI: Bringing Low Power to Wi-Fi Transmissions. *GetMobile: Mobile Computing and Communications* 20, 3: 38–41. https://doi.org/10.1145/3036699.3036711

25. Jungsoo Kim, Jiasheng He, Kent Lyons, and Thad Starner. 2007. The Gesture Watch: A wireless contact-free Gesture based wrist interface. In *Proceedings - International Symposium on Wearable Computers, ISWC*, 15–22. https://doi.org/10.1109/ISWC.2007.4373770

26. Kwangtaek Kim, Joongrock Kim, Jaesung Choi, Junghyun Kim, and Sangyoun Lee. 2015. Depth camera-based 3D hand gesture controls with immersive tactile feedback for natural mid-air gesture interactions. *Sensors (Switzerland)* 15, 1: 1022–1046. https://doi.org/10.3390/s150101022

27. Alexander O. Korotkevich, Zhanna S. Galochkina, Olga Lavrova, and Evangelos A. Coutsias. 2015. On the comparison of energy sources: Feasibility of radio frequency and ambient light harvesting. *Renewable Energy* 81: 804–807. https://doi.org/10.1016/j.renene.2015.03.065

28. Sven Kratz and Michael Rohs. 2009. Hoverflow: exploring around-device interaction with IR distance sensors. *… on Human-Computer Interaction with Mobile Devices …*, Figure 1: 1–4. https://doi.org/10.1145/1613858.1613912

29. Tianxing Li, Qiang Liu and Xia Zhou. 2017. Ultra-Low Power Gaze Tracking for Virtual Reality. In *the 15th ACM Conference on Embedded Network Sensor Systems (SenSys '17)*. https://doi.org/https://doi.org/10.1145/3131672.3131682

30. Tianxing Li, Chuankai An, Zhao Tian, Andrew T. Campbell, and Xia Zhou. 2015. Human Sensing Using Visible Light Communication. In *Proceedings of the 21st Annual International Conference on Mobile Computing and Networking - MobiCom '15*, 331–344. https://doi.org/10.1145/2789168.2790110

31. Tianxing Li, Qiang Liu, and Xia Zhou. 2016. Practical Human Sensing in the Light. In *Proceedings of the 14th Annual International Conference on Mobile Systems, Applications, and Services - MobiSys '16*, 71–84. https://doi.org/10.1145/2906388.2906401

32. Yi Li. 2012. Hand gesture recognition using Kinect. *Software Engineering and Service Science (ICSESS), 2012 IEEE 3rd International Conference on*: 196–199. https://doi.org/10.1109/ICSESS.2012.6269439

33. Jaime Lien, Nicholas Gillian, M Emre Karagozler, Patrick Amihood, Carsten Schwesig, Erik Olson, Hakim Raja, Ivan Poupyrev, and Google Atap. 2016. Soli: Ubiquitous Gesture Sensing with Millimeter Wave Radar. *ACM Trans. Graph. Article* 35, 10: 1–19. https://doi.org/10.1145/2897824.2925953

34. Mingyu Liu, Mathieu Nancel, and Daniel Vogel. 2015. Gunslinger: Subtle Arms-Down Mid-Air Interaction. In *Proceedings of the 28th Annual ACM Symposium on User Interface Software & Technology - UIST '15*, 63–71. https://doi.org/10.1145/2807442.2807489

35. Shenwei Liu and F Guimbretière. 2012. FlexAura: a flexible near-surface range sensor. *Proc. UIST*. https://doi.org/10.1145/2380116.2380158

36. Shang Ma, Qiong Liu, and Phillip C.Y. Sheu. 2018. Foglight: Visible Light-Enabled Indoor Localization System for Low-Power IoT Devices. *IEEE Internet of Things Journal* 5, 1: 175–185. https://doi.org/10.1109/JIOT.2017.2776964

37. Anders Markussen, Mikkel Rønne Jakobsen, and Kasper Hornbæk. 2014. Vulture: a mid-air word-gesture keyboard. *Proceedings of the 32nd annual ACM conference on Human factors in computing systems - CHI '14*: 1073–1082. https://doi.org/10.1145/2556288.2556964

38. A Mayberry, Y Tun, P Hu, D Smith-Freedman, D Ganesan, B M Marlin, and C Salthouse. 2015. CIDER: Enabling robustness-power tradeoffs on a computational eyeglass. *21st Annual International Conference on Mobile Computing and Networking, MobiCom 2015*. https://doi.org/10.1145/2789168.2790096

39. John Mulgrew, Bernard, Grant, Peter, Thompson. 2002. *Digital Signal Processing: Concepts and Applications*.

40. Saman Naderiparizi, Aaron N. Parks, Zerina Kapetanovic, Benjamin Ransford, and Joshua R. Smith. 2015. WISPCam: A battery-free RFID camera. In *2015 IEEE International Conference on RFID, RFID 2015*. https://doi.org/10.1109/RFID.2015.7113088

41. Shree K. Nayar, Daniel C. Sims, and Mikhail Fridberg. 2015. Towards Self-Powered Cameras. In *2015 IEEE International Conference on Computational Photography, ICCP 2015 - Proceedings*. https://doi.org/10.1109/ICCPHOT.2015.7168377

42. P. H. Niemenlehto. 2009. Constant false alarm rate

detection of saccadic eye movements in electro-oculography. *Computer Methods and Programs in Biomedicine* 96, 2: 158–171. https://doi.org/10.1016/j.cmpb.2009.04.011

43. Masa Ogata, Yuta Sugiura, Hirotaka Osawa, and Michita Imai. 2012. iRing: Intelligent Ring Using Infrared Reflection. In *Proceedings of the 25th annual ACM symposium on User interface software and technology - UIST '12*, 131–136. https://doi.org/10.1145/2380116.2380135

44. Parth H. Pathak, Xiaotao Feng, Pengfei Hu, and Prasant Mohapatra. 2015. Visible Light Communication, Networking, and Sensing: A Survey, Potential and Challenges. *IEEE Communications Surveys and Tutorials* 17, 2047–2077. https://doi.org/10.1109/COMST.2015.2476474

45. Qifan Pu, Sidhant Gupta, Shyamnath Gollakota, and Shwetak Patel. 2013. Whole-home gesture recognition using wireless signals. In *Proceedings of the 19th annual international conference on Mobile computing & networking - MobiCom '13*, 27. https://doi.org/10.1145/2500423.2500436

46. Dongseok Ryu, Dugan Um, Philip Tanofsky, Do Hyong Koh, Young Sam Ryu, and Sungchul Kang. 2010. T-less: A novel touchless human-machine interface based on infrared proximity sensing. In *IEEE/RSJ 2010 International Conference on Intelligent Robots and Systems, IROS 2010 - Conference Proceedings*, 5220–5225. https://doi.org/10.1109/IROS.2010.5649433

47. C. Scharf, L. L., Demeure. 1991. *Statistical signal processing: detection, estimation, and time series analysis*. Addison-Wesley Reading, MA.

48. Jie Song, Gábor Sörös, Fabrizio Pece, Sean Ryan Fanello, Shahram Izadi, Cem Keskin, and Otmar Hilliges. 2014. In-air gestures around unmodified mobile devices. In *Proceedings of the 27th annual ACM symposium on User interface software and technology - UIST '14*, 319–329. https://doi.org/10.1145/2642918.2647373

49. Li Sun, Souvik Sen, Dimitrios Koutsonikolas, and Kyu-Han Kim. 2015. WiDraw: Enabling Hands-free Drawing in the Air on Commodity WiFi Devices. In *Proceedings of the 21st Annual International Conference on Mobile Computing and Networking - MobiCom '15*, 77–89. https://doi.org/10.1145/2789168.2790129

50. Vamsi Talla, Bryce Kellogg, Shyamnath Gollakota, and Joshua R. Smith. 2017. Battery-Free Cellphone. *Proceedings of the ACM on Interactive, Mobile, Wearable and Ubiquitous Technologies* 1, 2: 1–20. https://doi.org/10.1145/3090090

51. Danhang Tang, Tsz Ho Yu, and Tae Kyun Kim. 2013. Real-time articulated hand pose estimation using semi-supervised transductive regression forests. In *Proceedings of the IEEE International Conference on Computer Vision*, 3224–3231. https://doi.org/10.1109/ICCV.2013.400

52. Thorlab. Photodiode Tutorial.

53. Hoang Truong, Phuc Nguyen, Anh Nguyen, Nam Bui, and Tam Vu. 2017. Capacitive Sensing 3D-printed Wristband for Enriched Hand Gesture Recognition. In *Proceedings of the 2017 Workshop on Wearable Systems and Applications - WearSys '17*, 11–15. https://doi.org/10.1145/3089351.3089359

54. Satoshi Tsuji. 2012. A tactile and proximity sensor by optical and electrical measurement. In *Proceedings of IEEE Sensors*. https://doi.org/10.1109/ICSENS.2012.6411050

55. Ambuj Varshney, Andreas Soleiman, Luca Mottola, and Thiemo Voigt. 2017. Battery-free Visible Light Sensing. In *Proceedings of the 4th ACM Workshop on Visible Light Communication Systems - VLCS '17*, 3–8. https://doi.org/10.1145/3129881.3129890

56. R. J.M. Vullers, R. van Schaijk, I. Doms, C. Van Hoof, and R. Mertens. 2009. Micropower energy harvesting. *Solid-State Electronics*. https://doi.org/10.1016/j.sse.2008.12.011

57. Juan Pablo Wachs, Mathias Kölsch, Helman Stern, and Yael Edan. 2011. Vision-based hand-gesture applications. *Communications of the ACM* 54, 2: 60. https://doi.org/10.1145/1897816.1897838

58. Anusha Withana, Roshan Peiris, Nipuna Samarasekara, and Suranga Nanayakkara. 2015. zSense: Enabling Shallow Depth Gesture Recognition for Greater Input Expressivity on Smart Wearables. *Proceedings of the ACM CHI'15 Conference on Human Factors in Computing Systems* 1: 3661–3670. https://doi.org/10.1145/2702123.2702371

59. Xing-Dong Yang, Tovi Grossman, Daniel Wigdor, and George Fitzmaurice. 2012. Magic Finger: Always-Available Input through Finger Instrumentation. *Proceedings of the 25th annual ACM symposium on User interface software and technology - UIST '12*: 147–156. https://doi.org/10.1145/2380116.2380137

60. Liang Yin, Xiping Wu, and Harald Haas. 2016. Indoor visible light positioning with angle diversity transmitter. In *2015 IEEE 82nd Vehicular Technology Conference, VTC Fall 2015 - Proceedings*. https://doi.org/10.1109/VTCFall.2015.7390984

61. Bei Yuan and Eelke Folmer. 2008. Blind hero: enabling guitar hero for the visually impaired. *Proceedings of the 10th international ACM SIGACCESS conference on Computers and accessibility*: 169–176. https://doi.org/10.1145/1414471.1414503

62. Chi Zhang, Josh Tabor, Jialiang Zhang, and Xinyu Zhang. 2015. Extending Mobile Interaction Through Near-Field Visible Light Sensing. In *Proceedings of the 21st Annual International Conference on Mobile*

*Computing and Networking - MobiCom '15*, 345–357. https://doi.org/10.1145/2789168.2790115

63. Chi Zhang and Xinyu Zhang. 2016. LiTell: Robust Indoor Localization Using Unmodified Light Fixtures. *Proceedings of the 22nd Annual International Conference on Mobile Computing and Networking - MobiCom '16*: 230–242. https://doi.org/10.1145/2973750.2973767

64. Chen Zhao, Ke-Yu Chen, Md Tanvir Islam Aumi, Shwetak Patel, and Matthew S. Reynolds. 2014. SideSwipe. In *Proceedings of the 27th annual ACM symposium on User interface software and technology - UIST '14*, 527–534. https://doi.org/10.1145/2642918.2647380

65. Xia Zhou and Andrew T. Campbell. 2014. Visible light networking and sensing. *HotWireless 2014 - Proceedings of the 1st ACM MobiCom Workshop on Hot Topics in Wireless*: 55–59. https://doi.org/10.1145/2643614.2643621

66. BPW34. https://www.osram.com/os/ecat/DIL%20SMT%20BPW%2034%20S/com/en/class_pim_web_catalog_103489/global/prd_pim_device_2219543/.

67. ADG736. http://www.analog.com/media/en/technical-documentation/data-sheets/ADG736.pdf.

68. 74HC4514. http://www.ti.com/lit/ds/schs280c/schs280c.pdf.

69. LTC3106. http://www.analog.com/en/products/power-management/energy-harvesting/ltc3106.html.

70. MINI-M4 for MSP432. https://www.mikroe.com/mini-msp432.

71. MSP432P401R. http://www.ti.com/lit/ds/symlink/msp432p401r.pdf.

72. Monsoon. http://msoon.github.io/powermonitor/PowerTool/doc/Power%20Monitor%20Manual.pdf.

73. TS881. http://www.st.com/resource/en/datasheet/ts881.pdf.

74. Xbox Kinect. https://www.xbox.com/en-US/kinect.

75. Leap Motion. https://www.leapmotion.com/.

76. Point Grab. http://www.pointgrab.com/.

77. Crunch Fish. http://crunchfish.com/.

78. APDS-9130. https://www.broadcom.com/products/optical-sensors/proximity-sensors/apds-9130.

79. APDS-9190. https://www.broadcom.com/products/optical-sensors/proximity-sensors/apds-9190.

80. ads7042. http://www.ti.com/lit/ds/symlink/ads7042.pdf.